PERGAMON

Journal of Structural Geology 22 (2000) 429–440

JOURNAL OF STRUCTURAL GEOLOGY

www.elsevier.nl/locate/jstrugeo

The multiple inverse method applied to meso-scale faults in mid-Quaternary fore-arc sediments near the triple trench junction off central Japan

Atsushi Yamaji

Division of Earth and Planetary Sciences, Kyoto University, Sakyo-ku, Kyoto 606-8502, Japan

Received 6 March 1999; accepted 22 September 1999

Abstract

The multiple inverse method for fault-slip data is applied to meso-scale faults observed in mid-Quaternary fore-arc sediments near the triple trench junction off the Boso Peninsula, Japan. Data from the Otadai, Umegase and Kokumoto Formations were processed, and three stresses were obtained as significant solutions: vertical, axial compression, and triaxial stresses with the σ_3 axis in WNW–ESE and NNE–SSW directions. The triaxial stresses were determined from the Otadai and Umegase data. However, the WNW–ESE tensile stress is not detected from the youngest, Kokumoto, suggesting that the stress is older than the formation. The area was subject to a WNW–ESE tensile stress ~1.2–1.0 Ma, but tensile direction changed to a NE–SW trend thereafter. The succession was simultaneous with a tectonic event in the landward slope of the Sagami Trough, suggesting that the subduction of the Philippine Sea plate affected the stresses in the overriding plate. The older tensile stress was probably a manifestation of the gravitational collapse of the Hayama–Mineoka ridge, which was growing parallel to the trough. The inferred stress history is concordant with the variation of plate convergence at the trough. © 2000 Elsevier Science Ltd. All rights reserved.

1. Introduction

Plate interactions and large-scale topography are the primary and secondary origins of lithospheric stresses (Zoback, 1992). Triple trench junctions are interesting because they cannot be stationary with respect to the overriding plate (McKenzie and Morgan, 1969), leading the fore-arc to experience time-dependent topography and plate convergence. The modern junction off the Boso Peninsula, central Japan, is where the Sagami Trough, Japan and Izu–Bonin Trenches meet (Fig. 1). Seismic profiles under the landward slope of the trough suggest variable plate convergence in the Quaternary: tectonic events at about 1.0 and 0.5 Ma are attributed to the convergence of the Philippine Sea plate (Nakamura et al., 1984, 1987).

Many meso-scale faults in the Miura–Boso area have been investigated by many researchers to infer paleostresses (Kakimi et al., 1966; Kodama, 1968; Kinugasa et al., 1969; The Minor Fault Research Group, 1973; Ogawa and Horiuchi, 1978; Angelier and Huchon, 1987). In this paper, the term 'meso-scale fault' is used for the faults whose displacements can be determined in a single outcrop. The previous researchers detected the change of tectonic regime at about 0.5 Ma, however, the event at 1.0 Ma was not identified in the meso-scale faults. A question arises accordingly: are the events recorded in the fault population not there? The area probably experienced polyphase tectonics in the Quaternary. Each phase of tectonic stresses affected a part of the fault population, resulting in heterogeneous fault-slip data. It is a difficult task to separate stresses because usual inverse methods assume that all faults moved in response to a single stress state (Engelder, 1992).

E-mail address: ayamaji@ip.media.kyoto-u.ac.jp (A. Yamaji).

0191-8141/00/$ - see front matter © 2000 Elsevier Science Ltd. All rights reserved.
PII: S0191-8141(99)00162-5

Recently, Mino and Yamaji (1999) used Armijo et al.'s (1982) approach to process heterogeneous fault-slip data obtained from the central Boso area. They divided the data by minimizing misfits between observed and predicted slip directions using Angelier's (1979, 1984) classic inverse method. The conclusion was that the data are formidably heterogeneous for this method.

Yamaji (2000) presents a new numerical method called the multiple inverse (MI) method for heterogeneous fault-slip data. In this paper, the method is applied to meso-scale faults collected by Mino and Yamaji (1999). Identified stress states correlate with a stratigraphic succession, suggesting the age of the stresses. The temporal variation allows us to discuss the mid-Quaternary stress history in the Boso area.

2. Geologic setting

The MI method (Yamaji, 2000) is applied to Mino and Yamaji's (1999) data from the mid-Quaternary Otadai, Umegase, and Kokumoto Formations (Mitsunashi et al., 1959) in the central Boso Peninsula (Fig. 2). They occupy the middle of the Kazusa Group. The group is as thick as 3000 m, but thins westward. In the study area, the Otadai and Umegase Formations are about 500 m thick, and the Kokumoto Formation is 300 m thick. The formations consist of alternating beds of sandstone and mudstone. Sedimentological studies show that the strata are fore-arc basin fill (Ito and Katsura, 1993) that dipped eastward when they were deposited (Tokuhashi, 1992), but dip NNW at present (Mitsunashi, 1973). Benthic fossils suggest that the formation was deposited hundreds of meters below the sea level, but gradually became shallower during deposition (Aoki, 1968). The Kazusa Group is blanketed by the Shimosa Group that deposited in non-marine or shallow marine environments (Tokuhashi and Kondo, 1989; Ito and Katsura, 1992; Okazaki and Masuda, 1992). Accordingly, the formations have been uplifted and unroofed by several hundred meters within the last million years.

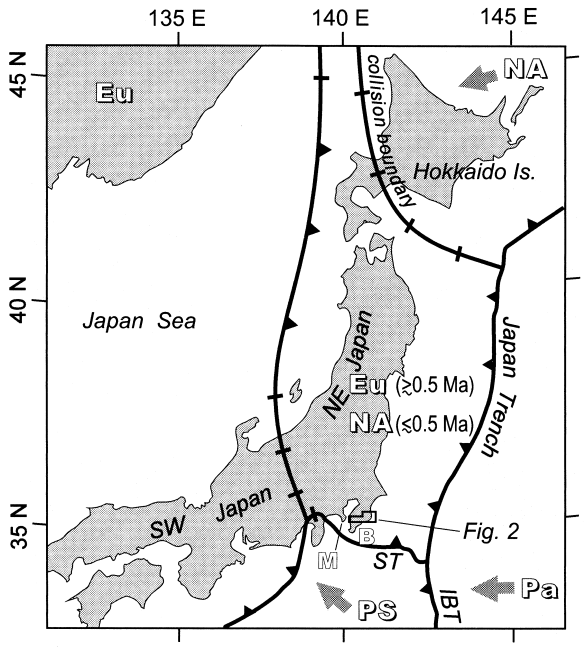

Fig. 1. Plate configuration around Japan. Boundary between North America and Eurasia jumped from northern Japan to the margin of Japan at around 0.5 Ma (Seno, 1988). Arrow: relative motion of plate with respect to Eurasia. Thick line: plate boundary. B: Boso Peninsula. Eu: Eurasia plate. IBT: Izu–Bonin Trench. M: Miura Peninsula. NA: North America plate. Pa: Pacific plate. PS: Philippine Sea plate. ST: Sagami Trough.

Magnetostratigraphy provides basic constraints for the age of the formations (Okada and Niitsuma, 1989). Cande and Kent's (1995) timescale is used in this study for the correlation of magneto- and chronostratigraphy. Paleomagnetic studies place the top of the Otadai Formation in the Jaramillo Event (0.99–1.07 Ma). Watanabe and Danhara (1996) integrated magnetostratigraphic, micropaleontologic and fission-track data and correlate the base of the Otadai Formation to the middle of the Matuyama Epoch. The base of the Brunhes Epoch (0.78 Ma) is found at the middle of the Kokumoto Formation. The top of the formation is estimated by oxygen isotope stratigraphy at about 0.7 Ma (Okada and Niitsuma, 1989). Recently, Masuda (1997) used sequence stratigraphy to correlate the Kazusa Group with well-dated strata to re-evaluate the age of the Kazusa Group. He correlated the base of the Otadai Formation at 1.2 Ma. Consequently, our fault-slip data were obtained from the horizon from about 0.7 to 1.2 Ma.

The lower Kazusa Group is cut by many N–S- to NNE–SSW-trending, moderately to steeply dipping faults with displacements of no more than tens of meters. Many key beds allowed Ishiwada et al. (1971) to trace minor faults with stratigraphic separation down to about 10 m. They found that the upper Kazusa Group is also affected by the faults, though they are rare in the horizon.

The formations are also cut by meso-scale faults. However, usually fewer than ten meso-scale faults are exposed at a single outcrop in the study area. This observation suggests a low intensity of the deformation affected the area. The Minor Fault Research Group (1973) observed hundreds of meso-scale to mappable faults in the lower Kazusa Group in the western Boso area. They traced many key beds and determined stratigraphic separations of the N–S- to NNE–SSW-trending faults. It was found that most fault blocks step down eastward and that the total subsidence of the key beds is about 0.5 km along E–W transects, 10–

20 km long. This indicates shear strain of about 0.5 km/10 km = 5%. They did not observe striae, so this is a very rough estimate.

3. Data

Because of the moderate deformation of the middle part of the Kazusa Group, Mino and Yamaji (1999) chose the area to investigate the methodology to separate stresses from heterogeneous data. The MI method is applied to the same data: 53, 29, and 20 data from the Otadai, Umegase, and Kokumoto Formations, respectively (Fig. 3). The method requires more than about 20 fault-slip data, though the lower limit depends on data. Therefore, data from each of the formations are collectively processed rather than from each of the outcrops.

The displacements of the meso-scale faults are less than a few meters. The three formations are composed of alternating beds of sandstone and mudstone, so that it is usually easy to determine the displacement and sense of slip. The faults have closed lips with fault gouge less than a few millimeters thick. Fig. 4 shows a typical meso-scale fault cutting turbidites of the Otadai Formation. Our data show that most of the faults in the formations are oblique-normal faults, but some are strike-slip faults (Fig. 3). The data are heterogeneous in that they cannot be explained by a single stress. For example, there are many NNE–SSW-trending oblique-slip faults with a variety of slip directions.

Fault block rotation leads stress inversion into error (Twiss and Unruh, 1998). In addition, it is usually difficult to determine the relative timing of stratal tilting and faulting. However, strata dip no more than 10° in the study area, so that the tilting of the faults is not corrected. The strata rotated during uplift, however, the following evidence confirms that the rotation is negligible. Paleocurrent (Ito and Katsura, 1993), lateral variation of thickness (Ito and Katsura, 1992), and paleobathymetry (Aoki, 1968) all indicate that the sedimentary basin opened eastward when the Kazusa Group was deposited. They suggest the paleoslope was around 2°. Therefore, we do not consider horizontal-axis rotation any more. Paleomagnetic data indicate that vertical-axis rotation is also negligible (Okada and Niitsuma, 1989).

4. Results

The MI method was applied first to the entire data set collected from the three formations. The detected significant stresses are represented by clusters of dot-

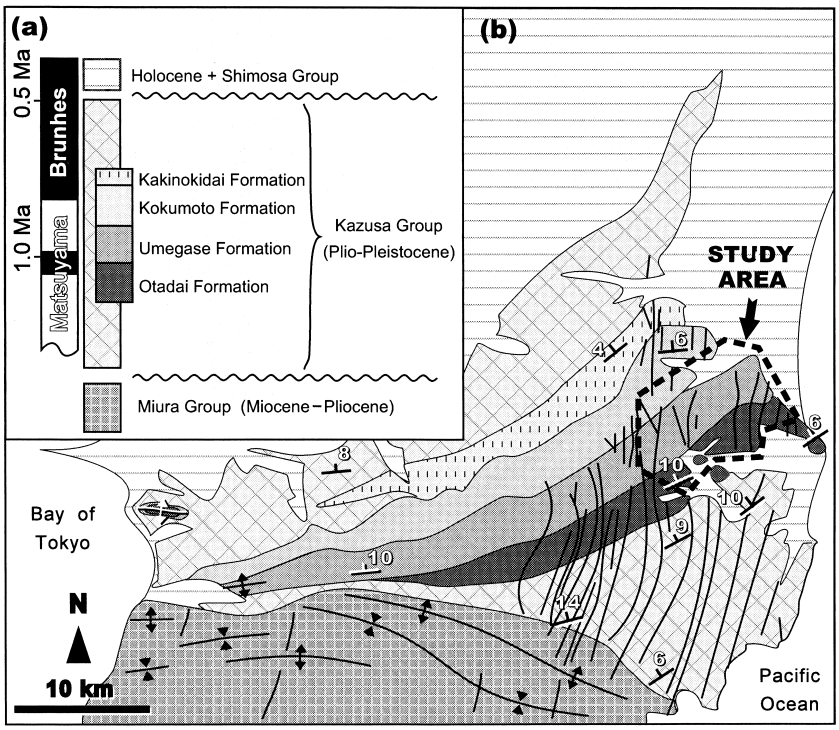

Fig. 2. (a) Quaternary stratigraphy of the central Boso area. Magnetostratigraphy after Okada and Niitsuma (1989). (b) Geologic map of the central part of the peninsula after Ishiwada et al. (1971) and Mitsunashi (1973). The Miura and lower Kazusa Groups are cut by a number of NNE–SSW-trending normal faults in the eastern part of the peninsula. The faults tip in the upper Kazusa Group. Most faults in the Miura Group are omitted in this figure for simplicity.

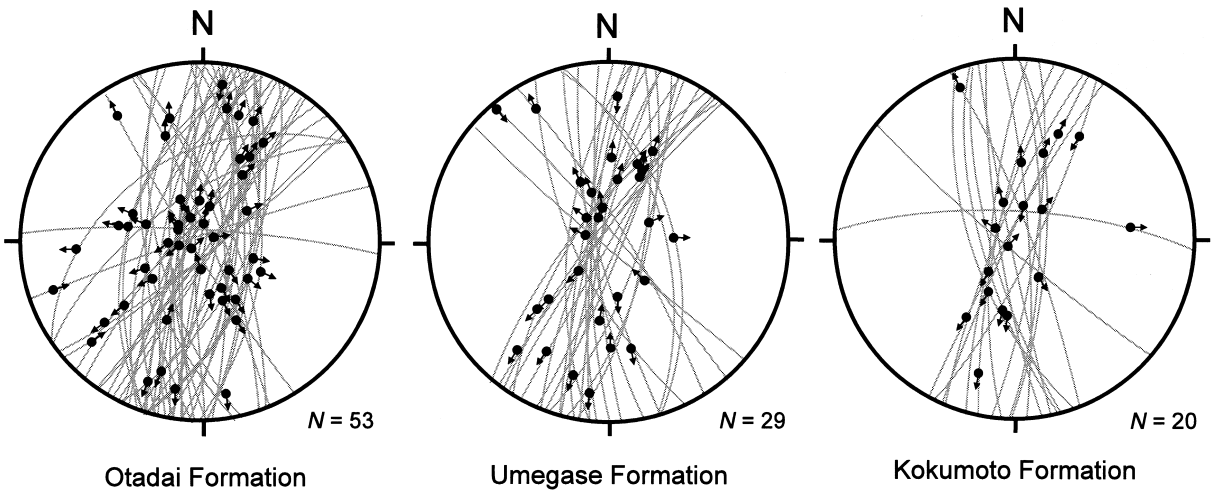

Fig. 3. Fault-slip data obtained from the Otadai, Umegase and Kokumoto Formations. Lower-hemisphere, equal-angle projection. Arrows show the slip direction of the hanging wall. Note that there are faults with similar orientations but with opposite sense, of movement, suggesting a polyphase stress regime.

and-bar symbols in an ordinary lower-hemisphere, equal-area projection (Fig. 5). The direction of the σ_3 axis is indicated by the position of a dot. The direction and length of the bar attached to the dot show the azimuth and plunge of the σ_1 axis of the stress state, respectively. The Lode number,

$$\mu_L = \frac{2\sigma_2 - \sigma_1 - \sigma_3}{\sigma_1 - \sigma_3}, \tag{1}$$

is shown by rainbow colors. This non-dimensional number indicates the shape of stress ellipsoid. Axial stresses are represented in Fig. 5 by violet ($\sigma_2 = \sigma_3$ and $\mu_L = -1$) and red ($\sigma_1 = \sigma_2$ and $\mu_L = 1$) symbols, and rainbow colors in between indicate triaxial stresses ($-1 < \mu_L < 1$).

4.1. Convergence of clusters

Given N data points, stress inversion is applied to a number of ${}_NC_k$ subsets of data, where

$${}_NC_k = \frac{N!}{k!(N-k)!} \tag{2}$$

Fig. 4. Typical meso-scale fault and lithofacies of the Otadai Formation.

is a binomial coefficient. The choice of a value for k is arbitrary—the optimal value depends on data. Smaller values of k make solutions unstable, whereas execution time for computation inflates with k. Accordingly, the optimal k is investigated. The parameter k was altered from 2 to 5 for the whole fault collection. In the case of $k = 2$, no dense cluster appears at all. By contrast, two clusters labeled as A and B stand out in Fig. 5 if $k \geq 3$. There is no significant difference in the clustering if $k \geq 4$, showing the convergence of solutions. The clusters obtained with $k = 3$ is more divergent than those with greater values of k. Consequently, $k = 4$ is the optimal choice for the whole data collection.

In order to help identify significant stresses, erroneous solutions should be thinned out to enhance correct ones. It is found from simulated and natural fault-slip data that the numerical density of solutions in four-dimensional parameter space obeys the relationship $\log P(m) \propto -\log m$, where m and $P(m)$ represent the density and the frequency distribution of the density, respectively (Yamaji, 2000) (Fig. 6). The distribution says that a great number of solutions gather at

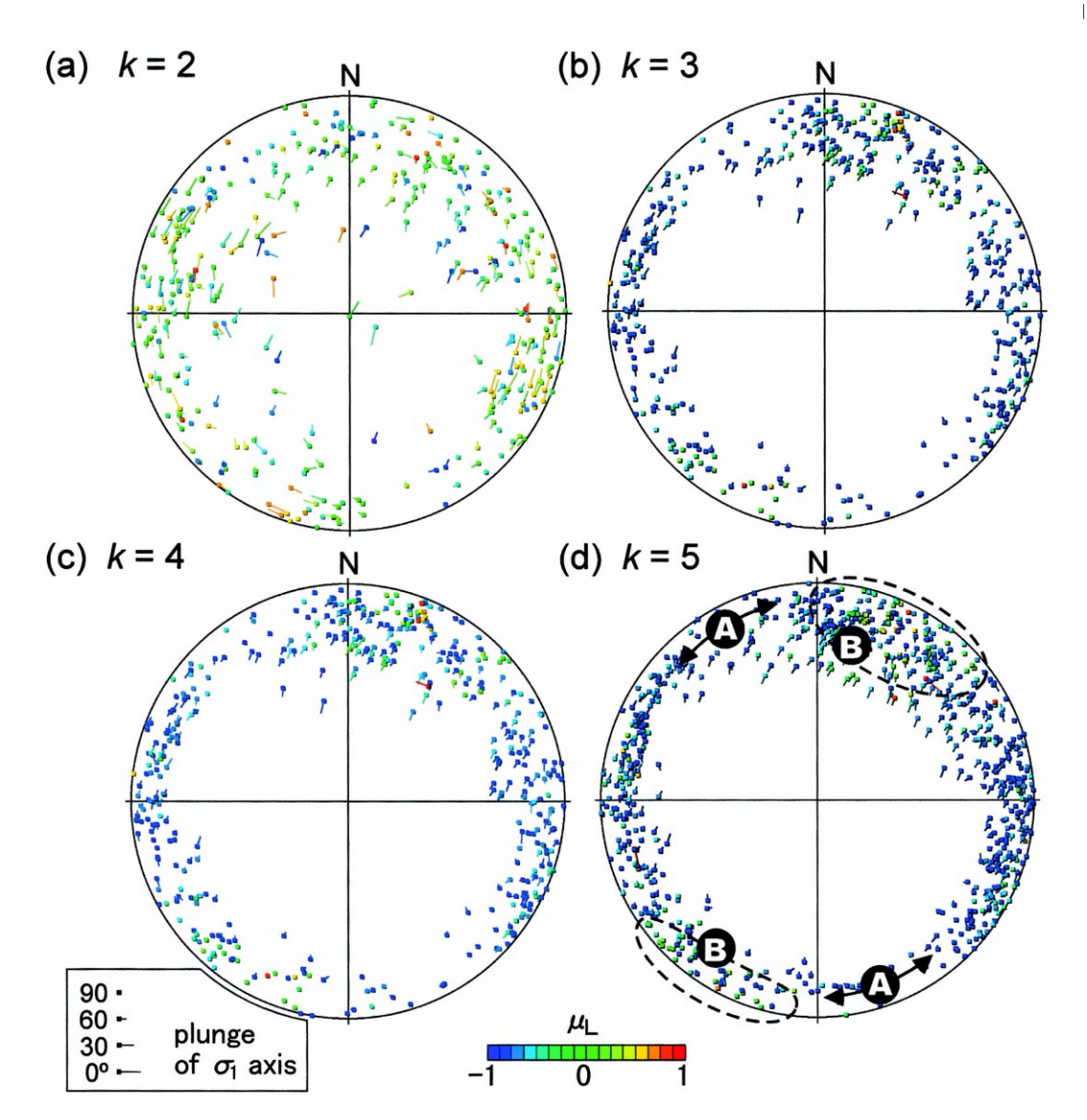

Fig. 5. Convergence of clusters derived by the MI method with $k = 2$–5 from the whole data set. Solutions of inverse calculation are represented by points in four-dimensional parameter space, and indicated by dot-and-bar symbols in these pictures. The direction of the σ_3 axis is shown by a dot on lower hemisphere, equal-area net, and that of the σ_1 axis is indicated by a bar attached to the dot: the azimuth and plunge of σ_1 is indicated by the direction and length of the bar, respectively. The length is proportional to the plunge. Lode number μ_L is color-coded. A cluster in the four-dimensional parameter space is visualized as a cluster of symbols with the same direction and length of bars, and with the same color. The enhancing factor is chosen at $e = 6$. There are two dominant clusters: the cluster of blue symbols, labeled as 'A', forms a great-circle girdle along the base circle. The green symbols clustering in the NE and SW quadrants are grouped as the cluster 'B'.

a small number of points in the parameter space—clusters appear. Accordingly, s, the standard deviation of m, can be used to thin out erroneous solutions: m/es symbols are plotted in Fig. 5, where the enhancing factor e is arbitrary, but is typically $e = 4$ or greater. If the quotient m/es is smaller than one, no symbol was drawn.

The cluster A in Fig. 5 is represented by the violet and blue symbols that make a great-circle girdle on the base circle. The colors indicate a very low stress ratio, so that it is approximately an axial stress with vertical σ_1 axis. Due to approximate horizontal isotropy, the blue dots that show the direction of σ_3 axes are distributed on the great circle. The violet and blue symbols have no or short bars attached, indicating vertical or steeply plunging σ_1 axes. Consequently, the cluster represents a stress with vertical axial compression, which we refer to as the stress A. The clusters of green symbols in the NE and SW quadrants are labeled as B, which represents a triaxial stress ($\mu_L \approx 0.0$) with NNE–SSW σ_3 and vertical σ_1 axes. This is called stress B.

The faults from the Otadai, Umegase, and Kokumoto Formations total 53, 29, and 20, respectively. The MI method was applied to each of the subgroups, and the results are shown in Fig. 7. Since the number of data is not large, the MI method was applied with k up to 7 to see the convergence of clusters. The stresses A, B, C and D were identified (Fig. 7). Stresses A and B are identical to those found from the whole fault collection. The stress C is represented by the clusters of green symbols, showing a vertical σ_1 and NW–SE-trending σ_3 axis with $\mu_L \approx 0.0$. The stress D is an axial ($\mu_L = 1$) stress with a NNE–SSW-trending σ_3 axis, and is represented by red symbols in Fig. 7. The stress has axial symmetry around the σ_3 axis so that the direction of the σ_1 axis is indicated by the great-circle girdle with the pole parallel to the σ_3 axis. The cluster D is the least dense among the labeled clusters.

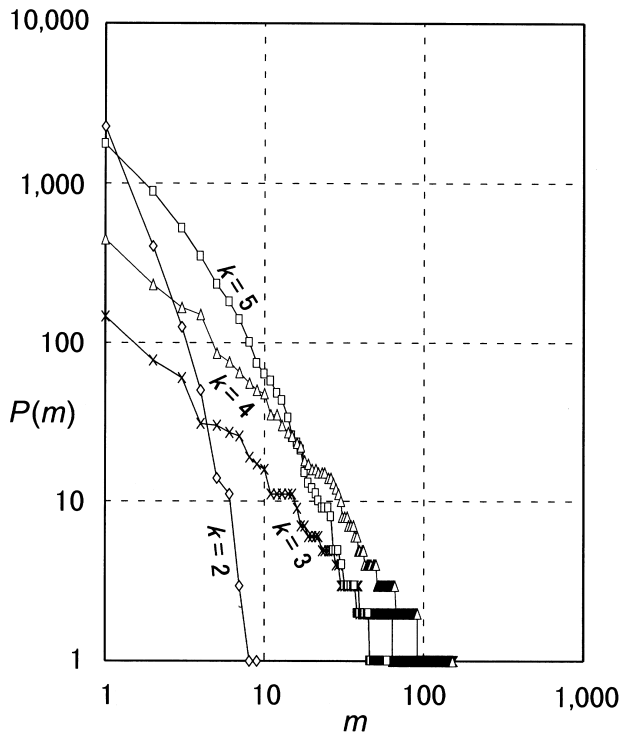

Fig. 6. Log–log plot of $P(m)$ for $k = 2$, 3, 4, and 5 where m stands for the number of solutions at a grid point in the four-dimensional parameter space, and $P(m)$ represents the frequency distribution of m.

It is notable that the clusters labeled C and D are absent in the results obtained from the Kokumoto and other data, respectively. The stresses A and B are identified from all the formations. Accordingly, the stresses A and B are enhanced when the MI method is applied to the whole fault collection, whereas the stresses C and D were hindered (Fig. 4).

5. Discussion

5.1. Methodology

Several methods have been proposed to process heterogeneous fault-slip data to identify stresses. Armijo et al. (1982) apply the classic inverse method recursively to those subsets of data that show large misfit from slip directions predicted from formerly determined stresses. The first inversion is applied to the whole fault collection. However, it is sometimes difficult to find a break in the histogram of misfits to divide data for following iteration. In addition, data are subdivided many times and later iterations use small parts of them, resulting in unstable solutions.

Mino and Yamaji (1999) attempted to separate stresses by the procedures from the same data set used in this work. They failed in separating the heterogeneous data from the Otadai and Umegase Formations, because solutions became unstable at the second iteration. However, they detected a stress by the first inversion from the Otadai data, similar to the stress A. The recursive approach was able to identify the stress that is represented by one of the densest clusters derived by the MI method. The same is true for the Umegase case—they identified a solution corresponding to the stress C. The Kokumoto data yielded the stresses B and A, the same result as with the present method except for the failure to detect the stress D. The MI method shows that the clustering pattern for the Kokumoto data is simpler than those for the Otadai and Umegase data (Fig. 6). Consequently, the Otadai and Umegase data are formidably heterogeneous for the recursive approach.

The present method has an advantage over the

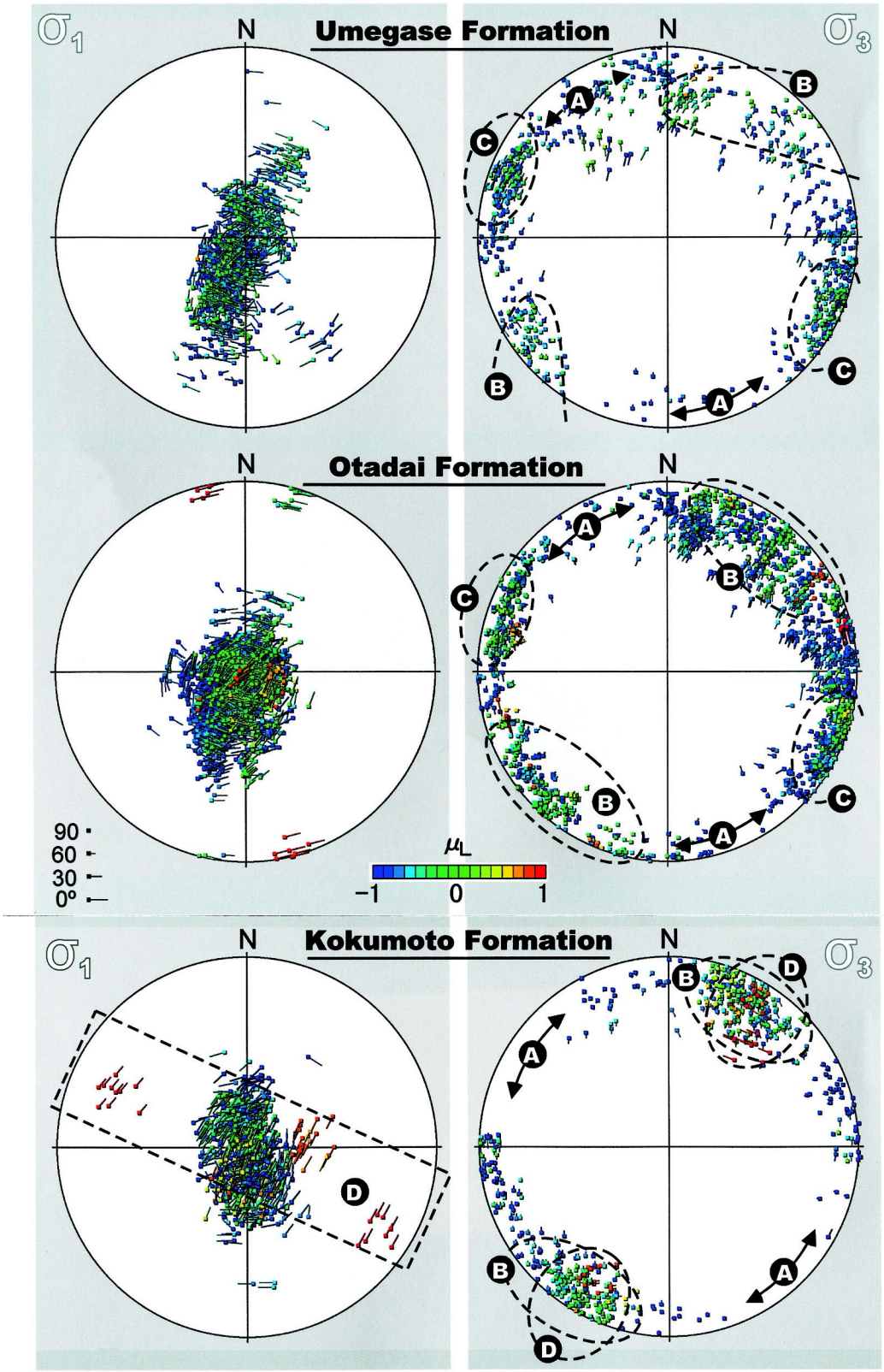

Fig. 7. Stresses identified by the MI method with $k = 7$ from the data of three formations. See Fig. 5 for legend. The clusters A, B, C and D stand out. The clusters A and B were also identified from the whole data set (Fig. 5). By contrast, the stress represented by the cluster C in the NE and SW quadrants is not identified from the Kokumoto Formation. The Kokumoto data yield the cluster of reddish symbols, labeled as D, showing NNE–SSW-trending, axial, deviatoric tension. The enhancing factor is chosen at $e = 4$ for the Kokumoto and Umegase data, and $e = 14$ for the Otadai data.

recursive method to study polyphase tectonics, as the former determines the optimal solutions with equal treatment. The recursive method divides data into subsets several times, so that later iterations use smaller numbers of data to determine optimal solutions. Solutions determined by later iteration are less reliable than earlier ones.

All inverse methods have limited resolution if observed faults have a small variation in their orientations. Given a fault set with a wide variety of orientations, it is easy for the MI method to detect correct stress(es). Unfortunately, most of the faults from which the present data were obtained have NNE–SSW to N–S strikes with steep dips, resulting in the difficulty to determine which stress is correct because they cause the faults to slip in similar directions. Such non-unique solutions appear typically in the cases in which we process conjugate faults. If a triaxial stress was responsible for the faulting, axial stresses with both $\mu_L = -1$ and $+1$ can appear as associated solutions as well as the triaxial stress (Yamaji, 2000). The stresses A and D identified from the Kokumoto data are typical examples, as the symmetry axis of the stresses A and D are parallel to the σ_1 and σ_3 axes of the triaxial stress B, respectively (Fig. 8). Among them, however, the slip directions by the axial stress D are somewhat different from those by the other stresses. Consequently, stress D is easier to separate than axial compression. This is reflected by the sparseness of the cluster D compared to those of A and B (Fig. 7). The stress D is therefore less significant and may be an artefact that appears as a shadow of the triaxial stress B. As a matter of fact, there are such axial deviatoric tensions whose symmetry axis is parallel to the σ_3 axis of the stresses B and C for the Otadai and Umegase cases. However, they are so sparse that they are thinned out in Fig. 7. Each of the triaxial stresses B and C has associating solutions of axial extension in different directions, so that the solutions make their shadows thin. In contrast, the axial compression that was referred to as the stress A has its σ_1 axis parallel to those of the triaxial stresses B and C, so that the axial compression is enhanced by the interference of them. There is only the triaxial stress B in the Kokumoto case, so that the axial extension D remained as well as the axial compression.

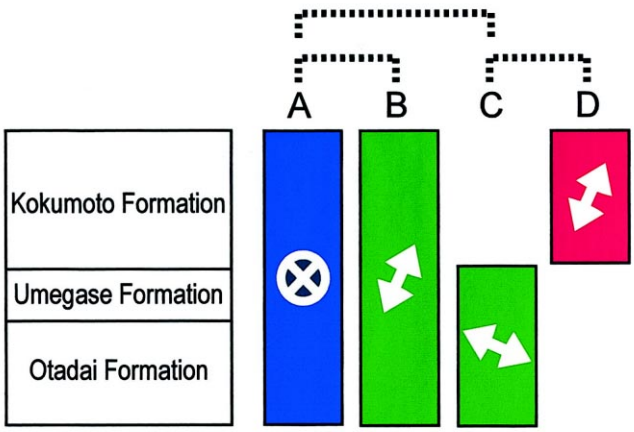

Fig. 8. Detected stresses A, B, C, and D, and their stratigraphic distribution. Stress A is vertical, axial compression. Stresses B and C are triaxial ($\mu_L \approx 0$) stresses with σ_3 axes in the NE–SW and WNW–ESE directions, respectively. Both stresses have vertical σ_1 and horizontal σ_3 axes. Stress D is horizontal axial deviatoric tension with the σ_3 axis in the NNE–SSW direction. Associated stresses are joined with dotted lines. Color indicates the Lode number of the stresses: violet $= -1$, green $= 0$, red $= +1$.

Conclusively, the triaxial stresses B and C are independent solutions (Fig. 8). The stress A may be an artefact caused by the two stresses, or a valid solution. The stress A allows various interpretations even if it is not an artefact. The solution is accounted by horizontally isotropic, tectonic extension and by compaction. Horizontally variable compaction in underlying strata may have been able to make growth faults with various orientations. The stress D is probably an artefact associated with the triaxial stress B.

5.2. Tectonic implications

Three stresses, A, B, and C, were identified in this study from the data obtained in the mid-Pleistocene strata (Fig. 8). The stress A was a vertical axial deviatoric compression ($\mu_L \approx -1.0$). The states B and C are triaxial stresses ($\mu_L \approx 0.0$) with NNE–SSW and WNW–ESE extension, respectively. They have a vertical σ_1 axis. None of the stresses is concordant with the present day compressive state (Tsukahara and Ikeda, 1987), indicating that they are paleostresses.

5.2.1. Age of stresses

Stratigraphic occurrence of the paleostresses suggests a chronology. All the stresses A, B and C are detected from the Otadai and Umegase Formations (Fig. 8). By contrast, the stresses A and B are separated from the Kokumoto data. The lack of the stress C in the youngest Kokumoto Formation suggests that the stress is older than the formation. Unfortunately, meso-scale faults are not so dense in the study area to allow verification of the relative age by the crosscutting relationship. Stratigraphic distribution of the stresses cannot be translated into time-distribution by themselves, however, the simultaneous tectonic events that are discussed in the following subsections support the inference. To be certain, we need more data around the study area or from subsurface strata.

The study area was probably subject to the stress state C when the Otadai and/or Umegase Formations were deposited. The stress was terminated at the top

of the Umegase stage just after the Jaramillo Event. During or after the accumulation of the Kokumoto Formation, the area was subject to stresses A and B. If the stress A was tectonic in origin, the stress might represent the transitional state from the stress state C to B. The stress A is equivocal, so I will not discuss it further.

5.2.2. Comparison with paleostresses detected by previous studies

Many researchers have studied meso-scale faults in the Boso and Miura Peninsulas. The stress C is probably identical to one of the stresses pointed out by those studies. However, the stress B is found for the first time. Kakimi et al. (1966) classified meso-scale faults in the Miura Peninsula according to their orientations, and suggest two stress states in the Quaternary: older N–S compression and younger NW–SE extension. Kodama (1968) observed slickenlines to verify the stresses. In the Boso area, Kinugasa et al. (1969) report a similar stress history. Those studies are based on Anderson's (1951) fault classification, therefore, they assumed that faults must compose conjugate sets. This is not always true. In the case where faults are dealt with as if they are conjugate faults but actually they are not, the conjugate hypothesis results in a complicated stress history as suggested by Kakimi (1974). Angelier and Huchon (1987) re-evaluated the stress history using the inverse method of Angelier (1984). As for Quaternary stress history, their conclusion agrees broadly with the 1960s' works, i.e. N–S compression was followed by NW–SE extension at about 1–2 Ma.

Our stress state C may be identical with Angelier and Huchon's (1987) younger extensional stress, although the correlation is not clear as they do not describe the plunge of stress axes nor the shape of stress ellipsoids. Since the Lode number of the stress C is near zero and the strike of the normal faults is more or less perpendicular to the σ_3 axis, the stress should have caused dip-slip normal faulting. Therefore, previous works that assumed conjugate faulting (Kakimi et al., 1966; Kodama, 1968; Kinugasa et al., 1969; The Minor Fault Research Group, 1973) pointed out correctly the stress axes of stress C. Kinugasa et al. (1969) used the macro-scale faults shown in Fig. 2 as well as meso-scale ones to demonstrate the stress. They were not able to detect the stress B.

The origin of the faults may be the joint system with those trends. There are two joint systems with NNE–SSW and E–W trends in the Miura Group that underlie the Kazusa Group to the south of the study area. The pre-existing, NNE–SSW-trending joints were activated as normal faults by the stress C, and parts of them were reactivated as oblique-normal faults by the stress B, causing fault activities in the overlying Kazusa Group.

The age of faulting is constrained by the observation that faults are rare in the upper Kazusa Group, which is younger than the Kokumoto Formation. Precise geologic mapping at a scale of 1:15 000 by Ishiwada et al. (1971) shows that N–S- to NNE–SSW-trending faults terminate mostly in the middle of the Kazusa Group; such faults are present but rare in the horizon younger than the Kasamori Formation, which blankets the Kokumoto Formation. A fission track age of 0.60 Ma is obtained from the Kasamori Formation (Watanabe and Danhara, 1996). The Kazusa Group is overlain by the Shimosa Group, which is composed by paralic sediments, and suffered little deformation by the faults (Kakimi, 1974). The base of the Shimosa Group yields radiometric ages of about 0.4 Ma (Tokuhashi et al., 1983; Shimokawa et al., 1992). Therefore, the stress state B was terminated by 0.5 ± 0.1 Ma.

Consequently, the study area was subject to the three stress states. The triaxial stress C with WNW–ESE-trending σ_3 axis was the oldest, and caused normal faulting from ~1.2 to 1.0 Ma. The stress A was vertical, axial compression, of unclear age. The stress A might be a transitional state from the stress C to B. The stress state B appeared in the area after the Jaramillo Event until ~0.5 Ma.

5.2.3. Implications for plate kinematics

Seismic profiles under the landward slope of the Sagami Trough revealed the transition in tectonic regime at about 1.0 Ma (Nakamura et al., 1987). The observation led Nakamura and his coworkers to suggest that the subduction direction of the Philippine Sea plate controlled tectonics in the overriding lithosphere. The event was simultaneous with the transition from the stress C to B (Fig. 9). Kotake (1988) finds a simultaneous event also in the southern tip of the Boso Peninsula. The Plio-Pleistocene Chikura Group is unconformably overlain by the upper Pleistocene Toyofusa Group, there. Kotake revealed that the area was subsiding in the Chikura stage but was gradually uplifted in the Toyofusa stage. The hiatus between the groups is correlated with the entire Otadai and possibly Umegase stages, and the upper bound of the hiatus is older than the Brunhes–Matuyama boundary (Kotake et al., 1995), same as the inferred age of the stress C.

The original interpretation by Kakimi et al. (1966) seems to be the most probable explanation for the extension. They suggested that the normal faulting represents the late stage activity of the growing Hayama–Mineoka ridge. The upper crust was transferred eastward by the normal faulting. There are a few faults that indicate extensional tectonics in the southern Boso area (Angelier and Huchon, 1987). The exten-

sional stress C affected only the Hayama–Mineoka ridge and its flanks. The southern Boso area was in a compressional stress regime at that time (Kotake, 1988). In the Futtsu area to the north of the ridge, E–W-trending folds were growing in the Otadai–Umegase stage (Yamauchi et al., 1990). To the north of the Miura Peninsula, normal faults are rare in the Yokohama area (Kakimi, 1974). In the Boso area to the east of Miura, the tensional zone was wider. The stress caused normal faulting that extended the upper crust eastward (Fig. 7). The fact is that most of the N–S- to NNE–SSW-trending normal faults dip eastward (Kinugasa et al., 1969; The Minor Fault Research Group, 1973).

The stress state C (WNW–ESE extension) was succeeded by the stress B (NNE–SSW extension) after

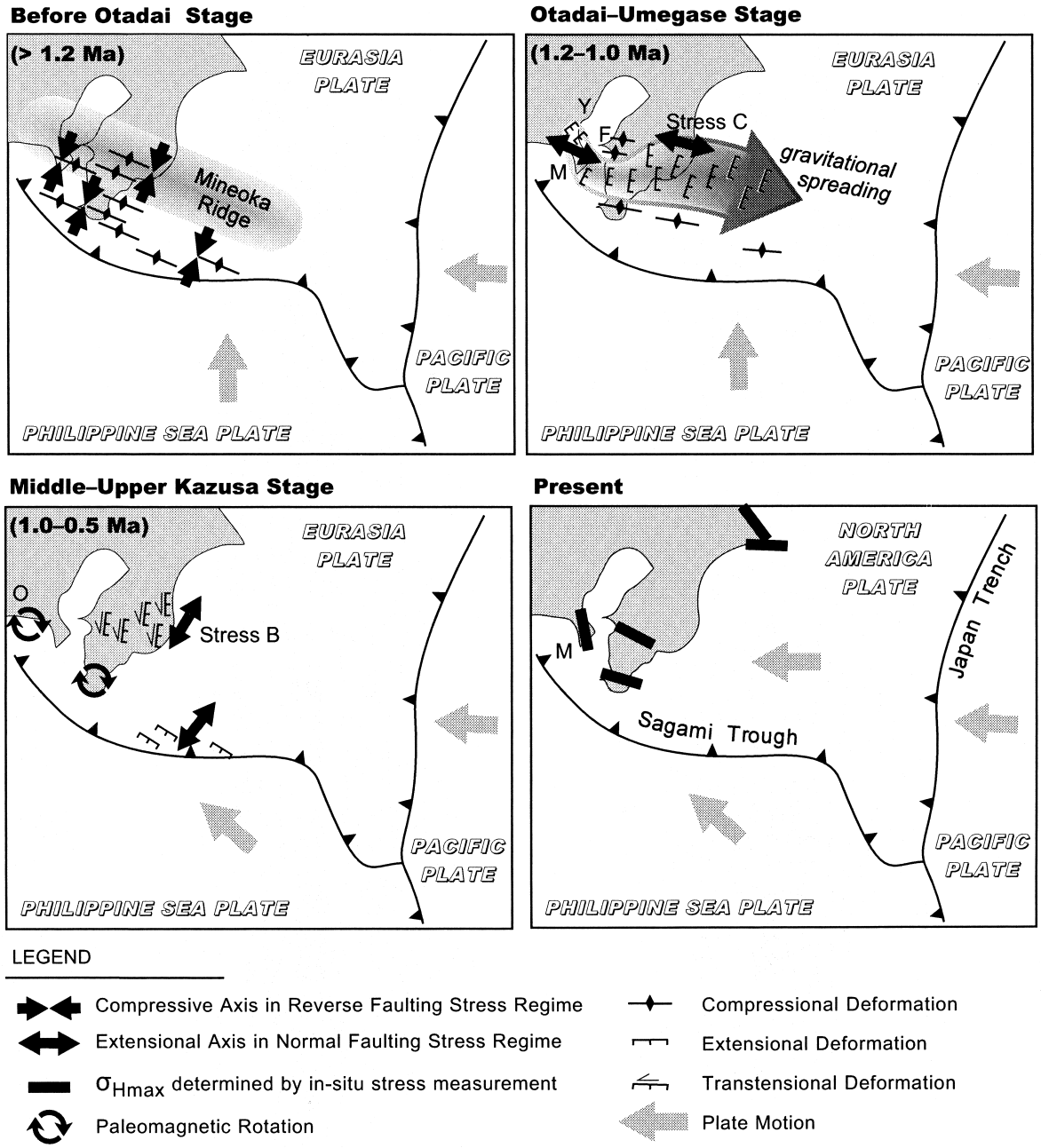

Fig. 9. Schematic to show the tectonic evolution around the Boso Peninsula. Quaternary stress field in the area is explained by three factors: (1) gravitational collapse of the growing Hayama–Mineoka ridge toward the Japan Trench, (2) the change of movement of the Philippine Sea plate, and (3) NE Japan's change of plates from the Eurasia to North America plate. F: Futtsu, M: Miura Peninsula, O: Oiso, Y: Yokohama. Data source: Angelier and Huchon (1987), Kakimi et al. (1966), Kodama (1968), Kotake et al. (1995), Koyama and Kitazato (1988), Tsukahara and Ikeda (1987). See text for detail.

1.0 Ma. Extensional direction rotated at about 90°. Nakamura et al. (1987) found grabens near the Sagami Trough that are concordant with the stress B. The grabens were shown to have formed after N–S compression. Nakamura and his coworkers (op. cit.) dated the transition at about 1.0 Ma, simultaneous with the rotation of the extensional direction in the central Boso area.

Nakamura et al. (1987) attributed the graben formation to the highly oblique subduction of the Philippine Sea plate at the Sagami Trough. They thought that the plate subducted at a higher angle before ca. 1.0 Ma. The timing is consistent with the change of subduction direction inferred by Yamazaki and Okamura (1989) who studied detailed submarine topography at the northern margin of the Philippine Sea plate. The highly oblique subduction between ~1.0 and 0.5 Ma is consistent with the timing of paleomagnetic rotation in the southern Boso (Kotake et al., 1995) and the Oiso areas (Koyama and Kitazato, 1988) (Fig. 9). Nakamura et al. (1987) suggest the clockwise rotation of the subduction direction at about 0.5 Ma to account for the youngest, compressional, minor structures around the Sagami Trough. Seno (1985) attributes the rotation to the behavior of NE Japan including the northern slope of the Sagami Trough: the NE Japan arc belonged to the Eurasia plate, which is almost stationary, but changed to the North America plate at that time, and began westward movement.

Acknowledgements

I thank F. Masuda, A. Okada, and K. Takemura for discussions, K. Mino for the permission to use the fault-slip data. Thanks are also due to J. M. Fletcher, J. P. Evans, L. Arlegui, A. F. Nieto-Samaniego, and T. Shimamoto for critical comments that were useful to improve the manuscript. Funded by the Grant-in-Aid for Scientific Research (08304033) from the Ministry of Education, Science and Culture, Japan.

References

Anderson, E.M., 1951. The Dynamics of Faulting and Dyke Formation with Application to Britain, 2nd ed. Oliver & Boyd, Edinburgh.

Angelier, J., 1979. Determination of the mean principal direction of stresses for a given fault population. Tectonophysics 56, T17–T26.

Angelier, J., 1984. Tectonic analysis of fault slip data sets. Journal of Geophysical Research 89, 5835–5848.

Angelier, J., Huchon, P., 1987. Tectonic record of convergence changes in a collision area: the Boso and Miura peninsulas, central Japan. Earth and Planetary Sciences Letters 81, 397–408.

Aoki, N., 1968. Benthic foraminiferal zonation of the Kazusa Group, Boso Peninsula. Transactions and Proceedings of the Paleontological Society of Japan, New Series 53, 163–169.

Armijo, R., Carey, E., Cisternas, A., 1982. The inverse problem in microtectonics and the separation of tectonic phases. Tectonophysics 82, 145–160.

Cande, S.C., Kent, D.V., 1995. Revised calibration of the geomagnetic polarity timescale for the Late Cretaceous and Cenozoic. Journal of Geophysical Research 100, 6093–6095.

Engelder, T., 1992. Stress regimes in the lithosphere. Princeton University Press, Princeton.

Ishiwada, Y., Mitsunashi, T., Shinada, Y., Makino, T., 1971. Geological maps of the oil and gas field of Japan; 10, Mobara. Geological Survey of Japan Map, scale 1:50,000.

Ito, M., Katsura, Y., 1992. Inferred glacio-eustatic control for high-frequency depositional sequences of the Plio-Pleistocene Kazusa Group, a forearc basin fill in Boso Peninsula, Japan. Sedimentary Geology 80, 67–75.

Ito, M., Katsura, Y., 1993. Depositional sequences in turbidite successions of the lower Kazusa Group, the Plio-Pleistocene forearc basin fill in the Boso Peninsula, Japan. Journal of the Geological Society of Japan 99, 813–829.

Kakimi, T., 1974. Quaternary stress history in the south Kanto district. In: Kakimi, T., Suzuki, Y. (Eds.), Seismic activities and tectonics of the Kanto district. Rateis, Tokyo, pp. 51–70.

Kakimi, T., Hirayama, J., Kageyama, K., 1966. Tectonic stress-field from the Minor fault systems in the northeastern part of the Miura Peninsula. Journal of the Geological Society of Japan 72, 469–489.

Kinugasa, Y., Kakimi, T., Hirayama, J., 1969. The minor-fault systems on the coastal area of the eastern Boso Peninsula. Bulletin of the Geological Survey of Japan 20, 13–38.

Kodama, K., 1968. An analytical study on the minor faults in the Jogashima Island. Journal of the Geological Society of Japan 74, 265–278.

Kotake, N., 1988. Upper Cenozoic marine sediments in southern part of the Boso Peninsula, central Japan. Journal of the Geological Society of Japan 94, 189–206.

Kotake, N., Koyama, M., Kameo, K., 1995. Magnetostratigraphy and biostratigraphy of the Plio-Pleistocene Chikura and Toyofusa Groups, southernmost part of the Boso Peninsula, central Japan. Journal of the Geological Society of Japan 101, 515–531.

Koyama, M., Kitazato, H., 1988. Paleomagnetic evidence for Pleistocene clockwise rotation in the Oiso Hills: a possible record of interaction between the Philippine Sea Plate and Northeast Japan. Rock Magnetism and Paleogeophysics 15, 35–38.

McKenzie, D., Morgan, W.J., 1969. Evolution of triple junction. Nature 224, 125–133.

Masuda, F., 1997. Correlation among oxygen isotope curves, the Shimosa and Kazusa Groups, and the Osaka Group: a preliminary note. Chikyu 19, 474–479.

Mino, K., Yamaji, A., 1999. The separation of paleostresses from heterogeneous fault-slip data: the case of Boso area, Japan. Journal of the Geological Society of Japan 105, 574–584.

Mitsunashi, T., 1973. Geologic Development of South Kanto and Niigata Sedimentary basins from Miocene to Pleistocene. Chikyu Kagaku 27, 48–65.

Mitsunashi, T., Yasukuni, N., Shinada, Y., 1959. Stratigraphical section of the Kazusa group along the shores of the rivers Yoro and Obitsu. Bulletin of the Geological Survey of Japan 10, 83–98.

Nakamura, K., Shimazaki, K., Yonekura, N., 1984. Subduction, bending and eduction. Present and Quaternary tectonics of the northern border of the Philippine Sea plate. Bulletin de la Societe des Sciences Naturelles de l'Ouest de la France 26, 221–243.

Nakamura, K., Renard, V., Angelier, J., Azema, J., Bourgois, J., Deplus, C., Fujioka, K., Hamano, Y., Huchon, P., Kinoshita, H., Labaume, P., Ogawa, Y., Seno, T., Takeuchi, A., Tanahashi, M., Uchiyama, A., Vigneresse, J.-L., 1987. Oblique and near collision

subduction, Sagami and Suruga Troughs—Preliminary results of the French–Japanese 1984 Kaiko cruise, Leg 2. Earth and Planetary Science Letters 83, 229–242.

Ogawa, Y., Horiuchi, K., 1978. Two types of accretionary fold belts in central Japan. Journal of Physics of the Earth 26, S321–S336.

Okada, M., Niitsuma, N., 1989. Detailed paleomagnetic records during the Brunhes–Matuyama geomagnetic reversal and a direct determination of depth lag for magnetization in marine sediments. Physics of the Earth and Planetary Interiors 56, 133–150.

Okazaki, H., Masuda, F., 1992. Depositional systems of the Late Pleistocene sediments in Paleo-Tokyo Bay area. Journal of the Geological Society of Japan 98, 235–258.

Seno, T., 1985. "Northern Honshu Microplate" hypothesis and tectonics in the surrounding region. Journal of the Geodetic Society of Japan 31, 106–123.

Seno, T., 1988. Philippine Sea plate kinematics. Modern Geology 14, 87–97.

Shimokawa, K., Imai, N., Nakazato, H., Mizuno, K., 1992. ESR dating of fossil shells in the middle to upper Pleistocene strata in Japan. Quaternary Science Reviews 11, 219–224.

The Minor Fault Research Group, 1973. A minor fault system around the Otaki area, Boso Peninsula, Japan. Chikyu Kagaku 27, 180–187.

Tokuhashi, S., 1992. Paleocurrent of the turbidite sandstones in the upper Pliocene Katsuura Formation of the lowermost Kazusa Group, Boso Peninsula, central Japan. Journal of the Geological Society of Japan 98, 943–952.

Tokuhashi, S., Danhara, T., Endo, H., Isoda, K., Nishimura, S., 1983. Experiments and problems on fission-track dating of geologically younger-age samples; with special reference to several volcanic ash layers in Kazusa and Shimosa groups, Boso Peninsula, central Japan. Bulletin of the Geological Survey of Japan 34, 241–269.

Tokuhashi, S., Kondo, Y., 1989. Sedimentary cycles and environments in the middle–late Pleistocene Shimosa Group, Boso Peninsula, central Japan. Journal of the Geological Society of Japan 95, 933–951.

Tsukahara, H., Ikeda, R., 1987. Hydraulic fracturing stress measurements and in-situ stress field in the Kanto-Tokai area, Japan. Tectonophysics 135, 329–345.

Twiss, R.J., Unruh, J.R., 1998. Analysis of fault slip inversions; do they constrain stress or strain rate? Journal of Geophysical Research 103, 12205–12222.

Watanabe, M., Danhara, T., 1996. Fission track ages of volcanic ash layers of the Kazusa Group in the Boso Peninsula, central Japan. Journal of the Geological Society of Japan 102, 545–556.

Yamaji, A., 2000. The multiple inverse method: a new technique to separate stresses from heterogeneous fault-slip data. Journal of Structural Geology, 22, 441–452.

Yamauchi, S., Mitsunashi, T., Okubo, S., 1990. Growth pattern of the Early Pleistocene Higashihigasa submarine channel, Boso Peninsula, central Japan. Journal of the Geological Society of Japan 96, 523–536.

Yamazaki, T., Okamura, Y., 1989. Subducting seamounts and deformation of overriding forearc wedges around Japan. Tectonophysics 160, 207–229.

Zoback, M.L., 1992. First- and second-order patterns of stress in the lithosphere: the World Stress Map Project. Journal of Geophysical Research 97, 11703–11728.